Commissioning of the First MRlinac in Latin America

Rojas-López José Alejandro[1,2], Cabrera-Santiago Alexis[3], González Souto Xesús[4]

[1]Hospital Almater SA de CV, [2]Facultad de Matemática, Astronomía, Física y Computación, Universidad Nacional de Córdoba, Córdoba, Argentina, [3]Unidad de Especialidades Médicas de Oncología, Mexicali, Baja California, México, [4]Elekta Inc., Atlanta, GA, USA

Abstract

Purpose: To show the workflow for the commissioning of a MRlinac, and some proposed tests; off-axis targets, output factors for small fields, dose in inhomogeneities, and multileaf collimator quality assurance (MLC QA). **Methods:** The tests were performed based on TG-142, TG-119, ICRU 97, TRS-398, and TRS-483 recommendations as well as national regulations for radiation protection and safety. **Results:** The imaging tests are in agreement with the protocols. The radiation isocenter was 0.34 mm, and for off-axis targets location was up to 0.88 mm. The dose profiles measured and calculated in treatment planning system (TPS) passed in all cases the gamma analysis of 2%/2 mm (global dose differences). The output factors of fields larger than 2 cm × 2 cm are in agreement with the model of the MRlinac in the TPS. However, for smaller fields, their differences are higher than 10%. Picket fence test for different gantry angles showed a maximum leaf deviation up to 0.2 mm. Displacements observed in treatment couch adding weight (50 kg) are lower than 1 mm. Cryostat, bridge, and couch attenuation was up to 1.2%, 10%, and 24%, respectively. **Conclusion:** The implemented tests confirm that the studied MRlinac agrees with the standards reported in the literature and that the strict tolerances established as a baseline should allow a smoother implementation of stereotactic treatments in this machine.

Keywords: Commissioning, MLC, MRlinac, output factors, SBRT

Introduction

The introduction of radiotherapy treatments guided by magnetic resonance imaging (MRgRT) is recent and has shown improvements in patient care, management of toxicities, and tumor control.[1] In our country, this technology is introduced for the first time with an Elekta Unity linac (MRlinac), integrated by a linear accelerator with 7 MV flattening-filter free photon beam, and a 1.5 T Philips magnetic resonance imaging (MRI) unit. However, the commissioning of this type of linac has additional complexity, since the effects introduced by magnetic fields in the beam influence the dosimetry parameters usually evaluated,[2] coupled with the current lack of specific international dosimetry protocols.

The MRlinac was installed in the hospital in May 2023, while acceptance testing, beam data collection, and onsite physics testing and commissioning were performed from August to October 2023. Clinical operation was habilitated in December 2023. This work shows the workflow for mechanical, dosimetric, and imaging tests implemented during the commissioning of a MRlinac to evince a rigorous process to use it clinically.

Methods

The following tests were performed based on international recommendations[3-5] and local radiation protection regulations.[6] Regarding reference and relative dosimetry, international code of practices TRS 398[7] and TRS-483[8] were followed, while the recommendations for dosimetry in the presence of magnetic fields by de Pooter[9] are considered.

Mechanical tests

Gantry angle

There are physical limitations to which gantry angles can be measured in the MRlinac, due to the location of the linac

Address for correspondence: Mr. Rojas-López José Alejandro, Hospital Almater SA de CV, Álvaro Obregón 1100, Segunda Sección, Mexicali, Baja California, México.
E-mail: alejandro.rojas@almater.com

How to cite this article: Alejandro RL, Alexis CS, Xesús GS. Commissioning of the first MRlinac in Latin America. J Med Phys 2024;49:213-224.

components on a ring. The recent recommendations to verify the gantry angle [10,11] were implemented.

In addition, an in-house phantom was built following the recommendations of Roberts *et al.*[12] to perform the star-shot test. The test was performed using a combination of six gantry angles, avoiding incidence with the edges of the table as recommended by Snyder *et al.*[11] Measurements were carried out with Gafchromic™ EBT4 film (Ashland, New Jersey, USA) irradiated with 500 UM per beam; the film was placed in a transverse plane and centered on the isocenter as shown in Figure 1a. The angles between the radiation beams were obtained using ImageJ software.

Elekta provides the MV alignment phantom (Elekta, Stockholm, Sweden), as shown in Figure 1b, which facilitates the implementation of several quality control tests, including the determination of the mechanical and radiation isocenter. This acrylic phantom was centered and aligned to the isocenter by means of the indexing bar guide; MV images were acquired using the linac MV imaging system (MVIC). Horizontal profiles of the images were obtained in ImageJ and the deviation between the maxima was considered as the mechanical variations. The deviation of the gantry angle was considered as the maximum deviation found for the pairs of angles.

MV isocenter determination

By the use of the cryostat characterization tool (CCT) shown in Figure 1c, Elekta performed the determination of the MV isocenter diameter. The analysis was performed by acquiring orthogonal images and they were processed with RIT Isocenter Analysis Tool v. 6.64 (Radiological Imaging Technologies, Colorado, USA).

Additionally, CCT was used to acquire orthogonal images with 3 cm × 3 cm fields delivering 100 UM. The images recorded in the MVIC were analyzed with free software QALMA[13] adjusting the distance to the isocenter to 143.5 cm. The two-dimensional (2D) deviations obtained were processed to
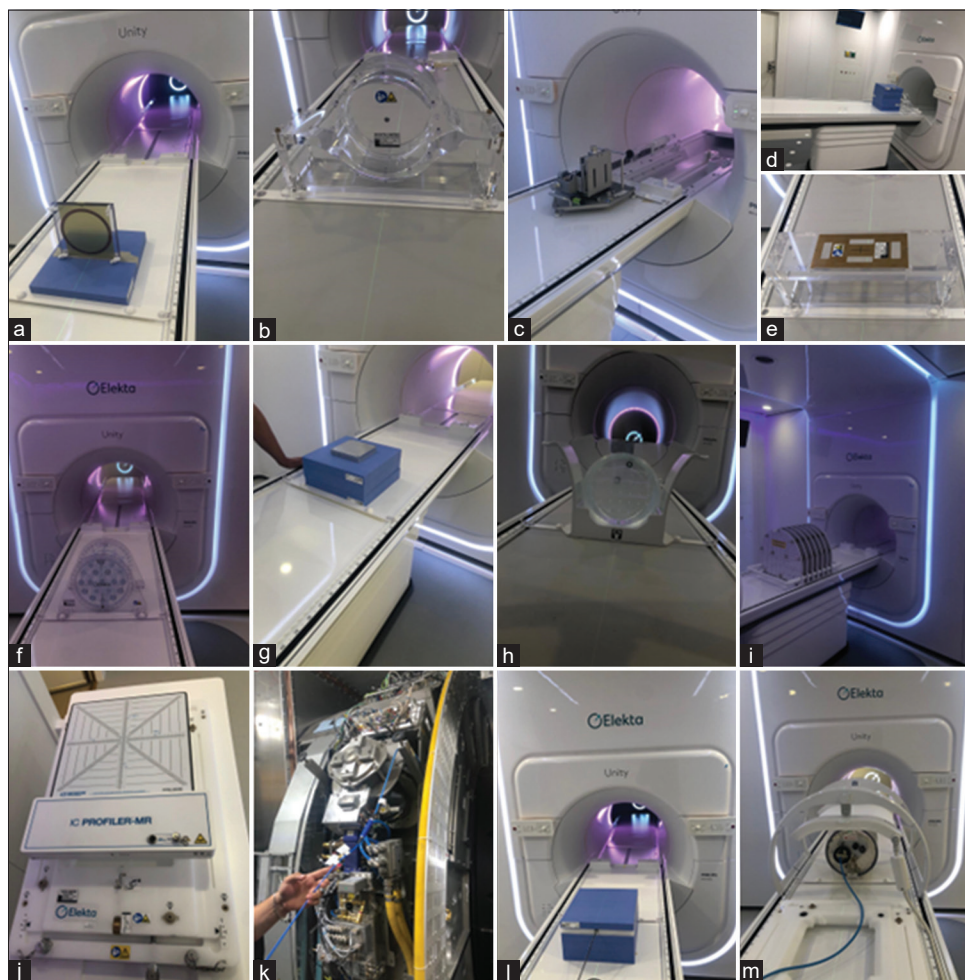

Figure 1: Experimental setup for the mechanical, imaging, and dosimetric tests. (a) Star-shot test and gantry angle. (b) mega voltage (MV) isocenter diameter and gantry angle. c) Off axis MV precision, and cryostat, table attenuation. (d) Table alignment with weight. (e) magnetic resonance (MRL) pixel plate tool. (f) magnetic resonance-to-MV phantom. (g) Las Vegas phantom setup. (h) Phantom for periodic image quality test for magnetic resonance images. (i) Geometric distortion phantom. (j) ionization chamber (IC) profiler for beam quality. (k) Setup for ionization chamber for reference in output factors for small beams. (l) Dose verification in inhomogeneities. (m) Computerized Imaging Reference Systems Inc (CIRS®) phantom for end-to-end test

determine the 3D deviation following the formalism of Low *et al.*[14]

AQUA® (Elekta, Stockholm, Sweden) is a web-based QA management solution that provides a single, access-controlled interface for scheduling, monitoring and reviewing all machine QA procedures and tasks. AQUA® software allows it to perform a similar test by taking eight images for a 5 cm × 5 cm field spaced every 45° using either the MV phantom or CCT. The 3D deviation from the isocenter was independently verified using the phantom in Figure 1b, acquiring the images described as above.

Finally, a star-shot test was performed using Gafchromic™ EBT4 and an Epson Expression 12000XL-GA scanner, using 48-bit at 72 dpi, in transmission mode. Image processing was performed in the free software Pylinac[15] with Python version 3.10.

MV off-axis determination

Once the 3D deviation from the isocenter was determined, the radiopaque ball bearing (BB) of the CCT was moved in the positive and negative directions along the X and Z axes (IEC61217 scale) up to a maximum of 3 cm, due to the physical limitations of the CCT. It was decided not to move in the Y direction since the movement of the table is in the cranial-caudal direction and possible deviations can be corrected in that direction.

The acquisition of four orthogonal images was carried out at the angles of 0º, 90º, 180º, and 270° with 3 cm × 3 cm fields displaced toward the direction where the CCT pointer moved. Images were further processed in ImageJ. The 2D deviation was defined in each axis as the distance between the pixels located at the center of the radiation field and at the center of the full width at half maximum (FWHM) of the CCT BB profile. The 3D deviation was obtained following the formalism of Low *et al.*[14] and the mathematical description described for off-axis targets in linacs.[16]

Treatment table accuracy

Since the MRlinac has no light field due to, it is not possible to verify the mechanical accuracy of the treatment table by using the light field, as is common in conventional linacs. Furthermore, it is necessary to characterize the precision of the table in the only direction of movement (in the cranial-caudal direction), since it is possible to find tilts that affect the treatments. For this reason, the phantom in Figure 1b was used, placing it in the most distal positions. Using table indexation and a relationship between indexes and table displacements, the phantom was brought to the isocenter. In these positions, orthogonal images (0°, 90°, 180° and 270°) were acquired with a field of 57 cm × 22 cm and 80 UM. Images were processed with STW Alignment software. The value delivered as deviation in the Y direction corresponds to the mechanical accuracy of the table. The test was repeated adding additional weight (50 kg) using slabs of solid water at the edges of the table, as shown in Figure 1d.

MLC calibration

During acceptance of MRlinac, the MLC calibration followed the workflow established by Elekta, similar to Agility MLC. The procedure consists of optical and radiation calibration. Additionally, the calibration of the MV panel is also required.

Elekta defines the leaf position as the radiological position. However, to define this, proper physical offset is required to provide exact leaf placement using the optical system. The optical calibration consists of a minor offset determination by mechanical diaphragm, camera tilt and skew, and leaf trajectory calibration. This minor offset is defined for each individual leaf, and it accounts for the physical distance from the detected ruby position to the physical leaf end.

The MV geometry calibration determines the electronic portal imager device (EPID) pixel pitch projected to isocenter as well as the pixel location of the MV isocenter projection on the panel. For the former, this procedure requires two images (gantry angle of 0° and 180°) of the MRL pixel plate tool [Figure 1e]. For the latter, the process consists of two parts: firstly, it is necessary to image the phantom on Figure 1b every 30° to determine the isocenter pixel IEC cross plane (X/Z) projection. Second, taking advantage of the V-shape of the back of the beam limiting device (BLD) diaphragms, it is possible to search for the center of the diaphragms and use this as a measure of the center of the radiation field along the Y axis of the EPID panel. This procedure is also performed every 30°, and the system records the pixel location of the isocenter projection on the MV panel for each of the analyzed gantry angles, as well as the mean value.

The radiation calibration consists of a major offset defining the absolute position of the MLC origin using a known landmark, and a major gain defining how the radiological projection changes with respect to the physical position as each MLC moves across the field.

For the major offset, the landmark used is the isocenter location defined during MV geometry calibration procedure. The pixel value of the isocenter projection for the gantry angle used during the MLC calibration (0°) is selected. Both the offset and the major gain are determined using a three-point calibration for central 24 leaves. The relationship between the physical and radiological position of the leaves is expressed as a straight line with parameters fitted from this three-point calibration, where the slope is the gain and the y-intercept is the offset previously described. Both parameters are applied to the whole leaf bank.

In addition, we performed the semi-automated routine to check the BLD performance, acquiring a set of rectangular fields varying the central axis offset to verify the position of the leaves. The analysis was made on Aqua software. As result, the positional error for all leaves is shown.

Finally, we executed two different Picket-Fence tests on iComCat software. The first one is the Bayouth (slit pattern) test that consists of irradiating a sequence of thick rectangular

bands (width 10 mm) separated by a fixed distance (10 mm) each.[17] The positioning accuracy of the leaves is verified through a dosimetric analysis of the position of the maximum and minimum doses in the sequence of bands. The second one is the Garden test that consists of irradiating a sequence of narrow rectangular bands (2 mm) separated by a distance of 2 cm each.[17] Due to its high sensitivity to positional variations, it was carried out by varying the gantry angle each time at 0°, 90°, 180° and 270°. The analysis was performed on Pylinac.

MR to MV coincidence isocenter

The distance between the MR image origin and radiation isocenter was measured using the Elekta MR-to-MV phantom, as shown in Figure 1f. This phantom consists of seven radio opaque zirconium oxide spheres of known geometry surrounded by a copper sulfate solution. Ten equidistant MV images of the phantom were taken, and a 3D reconstruction of the spheres is performed. Simultaneously, a 3D MRI of the phantom is taken. The position of the spheres is visible in the MRI as a void around the signal producing copper sulfate solution. The centers of all spheres were determined in both imaging modalities, and the detected positions were compared to calculate the 3D shift between both sets of images. The irradiated plan, MR acquisition T1 sequence and analysis software were provided by Elekta.

Imaging tests
Las Vegas test

The MVIC image quality was tested using Las Vegas phantom. It was placed at isocenter by the use of 14 cm solid water, as shown in Figure 1g. The image has good quality if it is easily identifiable at least 16 circles.

MR image quality

The flood field uniformity, spatial linearity, slice profile, and spatial resolution for different MR sequences were tested using the periodic image quality test (PIQT) and the corresponding phantom, as shown in Figure 1h, both provided by Philips. In order to evaluate the influence of artifacts produced by the linac components on the MR image, the test was repeated while the linac is on, the linac is off, the gantry is moving, and the MLC is moving.

Magnetic resonance imaging geometric distortion

Philips provides a phantom to evaluate the geometric distortion produced by the gradient coils on the MR image [Figure 1i]. The dimensions of the phantom are 500 mm × 375 mm × 330 mm. The MR markers are situated in seven planes separated by 55 mm and are spaced 25 mm apart within the plane.[11] The position of the markers was compared with the expected positions to produce a distortion map.

Additionally, the test was performed using the QUASAR™ MRI3D (IBA dosimetry, Schwarzenbruck, Germany) phantom during the acceptance tests positioning it on the bridge of the table and acquiring two MRI 3D fast field echo sequences. The analysis was performed on Quasar MRID 3D software using two spheres of 200- and 340-mm diameter. The thresholds

were mean 0.7 mm, max 1.5 mm, 5% above 1 mm, and mean 0.9 mm, max 3 mm, 5% above 2 mm, respectively.

Dosimetric tests
Beam data collection

The measurements were acquired in a BeamScan® 3D MR water tank (PTW, Freiburg, Germany) as established by Elekta acceptance procedure using a Semiflex 3D MR ionization chamber (PTW, Freiburg, Germany) and a MicroDiamond MR (PTW, Freiburg, Germany). This protocol establishes measurements at gantry at 0° for field sizes 2 cm × 2 cm, 3 cm × cm 3, 5 cm × 5 cm, 10 cm × 10 cm, 15 cm × 15 cm, 22 cm × 22 cm, 40 cm × 22 cm, and 57.4 cm × 22 cm up to 16 cm depth and at gantry angle of 270° for field sizes of 2 cm × 2 cm, 3 cm × 3 cm, 5 cm × 5 cm, 10 cm × 10 cm and 16 cm × 16 cm up to 30 cm depth. The measured curves were compared with Monaco treatment planning system (TPS) values using the Monaco Commissioning Utility software by gamma analysis of 2%/2 mm (global dose differences).

Additionally, depth dose profiles obtained in the TPS were compared with an independent Monte Carlo model.[18] The comparison was carried out using a grid spacing of 3 mm, 1% uncertainty per calculation point.

Reference dose

Prior to determine the reference dose, a cross-calibration was performed in a 6 MV Clinac iX linac (Varian, Palo Alto CA, United States) with flattening filter, and a Farmer TN30010 ionization chamber (PTW, Freiburg, Germany) using the isocentric technique. The objective of the cross-calibration was solely to validate the calibration factor for the MR compatible ionization chamber.

The reference dose was performed with an Exradin® A19 MR cylindrical chamber (Standard Imaging, Wisconsin, United States) and a PC Electrometer (Standard Imaging, Wisconsin, United States). The chamber was placed in a direction antiparallel to the magnetic field in a BeamScan® 3D MR water tank at a depth of 5 cm, with a gantry at 0° using a radiation field of 10×10 cm^2. The helium level at the time of calibration was 71.1%. The radiation beam was calibrated to deliver 1 MU per 1 cGy to the isocenter in these conditions. The dose was determined following de Pooter formalism, considering the magnetic field correction factor equal to $k_B = 1.005$. The $k_{Q, Q0}$ factor was equal to 0.987. This factor was calculated following the recommendations of Andreo *et al*.[19] Correction was performed for pressure, temperature, polarization, and ionic recombination.

Independent output validation provided by the MD Anderson Cancer Center Radiation Dosimetry Services (MDACC RDS) was examined. The thermoluminescent dosimeters (TLD) were irradiated with 300 MU and then mailed to the MDACC RDS for reading. For the measurement setup, wires were placed on the borders of the TLD cube phantom, and MV images were acquired by MVI without the cube. After the setup, the wires were removed and the TLD cube was placed. The

MDACC RDS uses geometric configuration, tissue maximum ratio (TMR) to determine the dose in the same conditions of irradiation at the reference dose. The TMR calculated in the TPS was equal to 0.9331.

Beam quality

Solid water slabs (SunNuclear, Melbourne FL, United States) were placed to measure doses at 10 cm and 20 cm depth, by isocentric technique. The holder for placing the cylindrical ionization chamber was filled with water to avoid dose perturbation with air cavities, as reported by O'Brien *et al*.[20] Subsequently, the quality of the beam by the TPR (20,10) was determined as the ratio between both measurements.

Similarly, the IC Profiler® (SunNuclear, Melbourne FL, United States) was used to determine the beam quality [Figure 1j]. For this purpose, it was placed centered on the isocenter as recommended by the manufacturer and solid water slabs were placed to give the depths of 10 cm and 20 cm (it was considered that the detector has 0.9 cm of equivalent water thickness). From the doses measured in the central detector, the TPR (20,10) was calculated.

Alternatively, through the depth dose curve, obtained at an angle of 0º with a field of 10×10 cm², the TPR (20,10) was determined using the equation on page 78 of TRS 398, which establishes the relationship between the dose at 10 cm depth, PDD (10), and the TPR (20,10), as shown in Equation 1. As recommended by TRS-398, this procedure helps to estimate the relationship between both parameters, but not to calibrate the accelerator.

$$TPR_{20,10} = -0.7898 + 0.0329PDD(10) - 0.00016PDD(10)^2. \quad (1)$$

Output factors

The output factors were measured in the central axis at 10 cm depth, at a 0º angle. A Semiflex 3D MR ionization chamber and a MicroDiamond MR, and the 3D BeamScan MR water tank were used to obtain the output factors. They were obtained for rectangular fields 57 cm × 22 cm, 40 cm × 22 cm, and square fields from 22 cm to 0.5 cm. In all cases, the reference chamber used was the Farmer type chamber Exradin® A19 MR placed adjacent to the linac head, as shown in Figure 1k. The values found are reported based on the nominal field size, S_{clin}, obtained as $S_{clin} = \sqrt{AB}$ where A and B are the FWHM of the inline and crossline profiles measured for each field. These values were obtained with the Semiflex chamber for fields larger than 5 cm and with the MicroDiamond for fields smaller than 5 cm.

Additionally, the output factors measured experimentally, and the corrected output factors, Ω, as recommended by the TRS-483[8] were compared with those calculated in the TPS. The calculated values were obtained using an equivalent water phantom of the same dimensions as the water tank, a spacing grid of 1 mm and 0.1% uncertainty per control point.

MLC transmission and dosimetric gap

The isocentric configuration was used, and 10 cm of solid water for backscatter was placed. We measured the dose at 5 cm depth, with a 10×10 cm² field and 200 UM, applying the correction factors indicated in point 2.2.1 with the ionization chamber oriented antiparallel to the magnetic field. Exradin® and Semiflex SNC125c (SunNuclear, Melbourne FL, United States) chambers were used. The measured dose was acquired using an open field, and, separately, for a field completely closed by the bank of leaves Y1, and Y2. The transmission by MLC or by jaws was obtained as the ratio of the measurement with respect to the open field. The measurements were compared with the calculated by the TPS. Monaco® TPS does not allow to cover the field only with the diaphragm. To make a field with only leaves, two open fields with the size of the minimum leaf gap were built at the corners of the maximum field.

Additionally, the dosimetric leaf gap (DLG) of the MLC was determined by generating beam sequences in iComCat with segments spaced 4, 6, 8, and 10 mm defined by the MLC with the experimental configuration described above. Subsequently, a linear fit was performed on the corrected measurements as described below. The value of the DLG is the one associated with a gap (g) equal to 0. The equation that allows to obtain the DLG is

$$M_{corr} = M_{raw} - \frac{T_{y1} + T_{y2}}{2}\left(1 - \frac{g(mm)}{100}\right), \quad (2)$$

where T_{y1} and T_{y2} is the MLC transmission for Y1 and Y2 banks, M_{raw} is the reading for the gap g (in mm).

Dose in inhomogeneities

Given that the effects of the interaction of charged particles in the presence of magnetic fields and in density inhomogeneities are known, the dose response was evaluated in a phantom with slabs of homogeneous (water) and inhomogeneous water-air-water density as shown in Figure 1l. A field of 10 cm × 10 cm and 100 UM was used at an angle of 0°. The point dose in the air was measured with the Exradin® chamber oriented antiparallel to the magnetic field and applying the correction factors in section 2.2.1.

The measured doses were compared with the doses calculated in the TPS under the same conditions using a grid spacing of 3 mm, 1% uncertainty per calculation point. Dosimetric calculation was performed on the 2.5 mm thick computed tomography (CT) images acquired on a CT LightSpeed VCT (GE, Boston MA, United States).

Cryostat and couch dose attenuation

As part of the linac acceptance tests, dosimetric characterization due to attenuation by the resonance cryostat is carried out. Measurements were obtained using CCT by placing a Farmer 30010 ionization chamber at the isocenter. To avoid disturbance of the dose by other elements of the linac, the bridge that allows the table to be supported inside the resonator bore was

removed. The CCT base was placed at the most distal edge of the table. The dose was measured by placing a cylindrical phantom with equivalent water thickness such that it guarantees electronic equilibrium in any direction, and the chamber cavity filled with water.

Subsequently, the attenuation produced by the bridge and the table was characterized, placing each of these elements in an experimental arrangement similar to that described above. In all cases, measurements were obtained every 2° and the values were normalized with respect to the dose at 90°.

Output versus gantry angle

Once the linac beam model was configured in the TPS, dose verification was performed using an ArcCheck®-MR (SunNuclear, Melbourne FL, United States). This phantom has a cylindrical geometry, and a Semiflex SNC125c ionization chamber can be placed at the center of the detector by the use of an acrylic holder. The chamber was inserted by placing liquid water to avoid air gaps inside the holder. The phantom is positioned on the treatment table using the QA Platform provided by Elekta.

The calculated dose was obtained at the center of the ionization chamber, in a set of 2.5 mm thickness CT images acquired on a CT LightSpeed VCT. The dose grid was 1 mm and 0.5% uncertainty per calculation point. The beams were configured to deliver 100 UM with a 10 cm × 10 cm square field equally spaced every 45°. The doses were normalized to the value obtained at 0°. The electron density assigned to the phantom was 1.220 and for the QA platform it was 1.350.

IMRT commissioning

As part of the Elekta beam validation procedure,[10] vendor IMRT plans, based on AAPM TG-119[4] guidance, were imported to the TPS and delivered on the MRlinac system. Elekta recommends gamma criteria of 3.0% (global dose difference) and 3.0 mm DTA during beam validation, with the ArcCheck®-MR device. The measurements for commissioning were evaluated using the clinical gamma criteria used in the hospital of 3.0%/2.0 mm, 2.0%/2.0 mm and 2.0%/1.0 mm (global dose differences).

The methodology for TPS calculation is provided below. Following clinical practice, TPS calculation for Elekta plans used a statistical uncertainty of 1.0% per calculation and a 3 mm dose grid. The calculated dose was set on ArcCheck®-MR CT images using a value of 1.220 for electronic density. To obtain these values, it was measured the entrance and exit doses for a 10 × 10 cm² field.

End-to-end test

During acceptance and commissioning, end-to-end test was performed using the CIRS ZEUS® MRgRT phantom (Sun Nuclear, Melbourne, Fl, USA), as shown in Figure 1m. The phantom was scanned in a LightSpeed VCT unit with 2.5 mm slice thickness. Additionally, T1 MR images were acquired directly on the Unity system to fuse with CT images for contouring. The images were merged in Monaco. PTV, liver and spinal cord were contoured.

The calculated dose deposition was performed to medium, using a dose grid of 3 mm, 1% of statistical uncertainty per calculation, a minimum segment area of 2 cm², and segment width of 5 mm. It used seven beams and an IMRT step-and-shot strategy. The dose prescription was 40 Gy in 20 fractions with dose coverage of 100% at 99%.

Since the ionization chamber is only MR conditional, having it in the bore during MR imaging could damage it. For this reason, the images were taken without the chamber, which was positioned in the field before the adapted plan was delivered. The phantom design includes an insert for the target with a chamber holder, which is easily detachable, thus ensuring the phantom position did not change during this process. The measured dose was acquired in a Semiflex 3D MR and correction factors were applied. The two possible workflows that can be performed in the Unity system were evaluated. The first one is adapt to position (ATP) and the second one is adapt to shape (ATS). For ATP no daily delineation is needed nor possible, and the dose calculation is performed in the pre-treatment CT with an updated isocenter location. However, for ATS the structure set can be re-contoured on the daily MR to be used for adapting the treatment plan, which is calculated in the MR with the updated anatomy.[21]

RESULTS

Mechanical tests

Gantry angle

The accuracy determined for the gantry angle is reported in Table 1. Images processed in ImageJ are shown in Figure 2.

MV isocenter determination

The radiation isocenter was determined by different methods and software, as shown in Table 2. In all cases the isocenter is <0.5 mm. Figure 3 shows the star shot analysis performed in Pylinac

MV off-axis determination

The deviation for targets located off axis far from isocenter in X and Z directions were determined. In Figure 4 it is represented that up to 3 cm, the maximum 3D deviation is 0.88 mm in Z direction.

Table 1: Gantry angle determination

Test	Spirit level	ImageJ by starshot image	ImageJ by opposite images
Value (°)	0.10	0.24	0.01

Table 2: Radiation isocenter determination

Test	RIT	QALMA	AQUA®	Pylinac
3D deviation (mm)	0.34	0.20	0.34	0.24

3D: Three dimensional, RIT: Radiological Imaging Technology, QALMA: Quality Assurance for Linac with Matlab
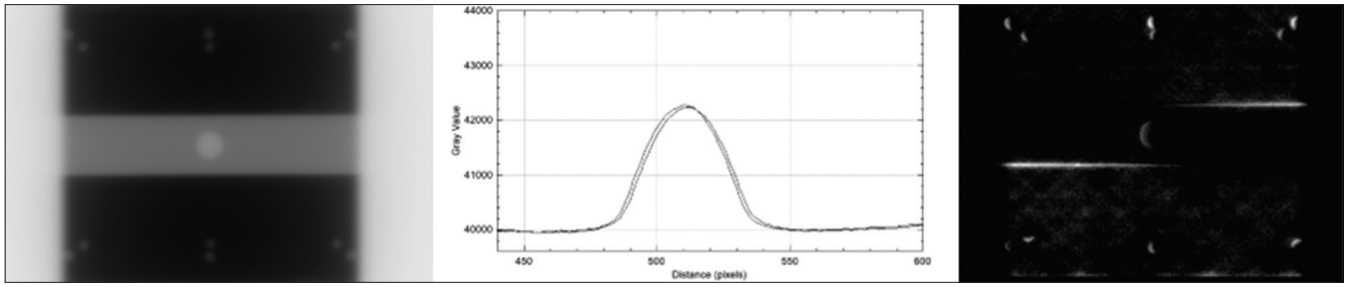
Figure 2: Analysis for opposite angle images in ImageJ. Left: Phantom image acquired at gantry 0°. Center: Plot profile at image center for images at gantry angle of 0° and 180°. Right: Image subtraction for gantry angle 0° and 180°. Hyperintense regions are related qualitatively with mechanical differences
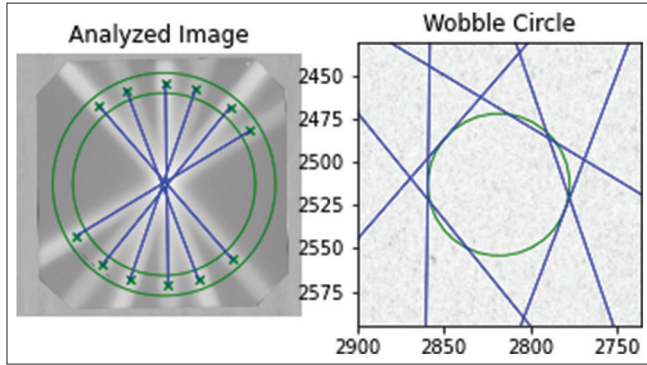

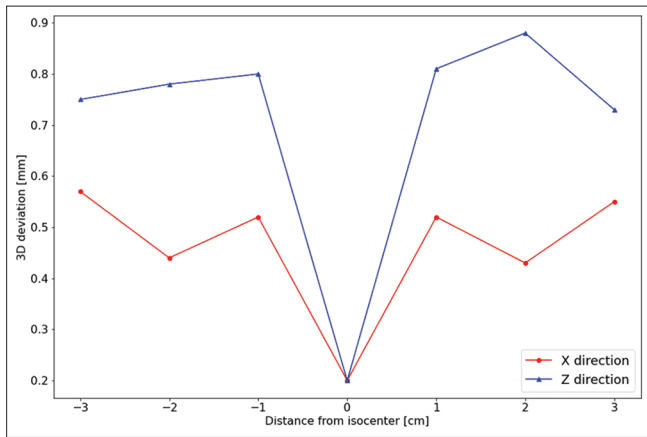**Figure 3:** Automated analysis in Pylinac for star shot test

Figure 4: Three-dimensional deviation of radiation isocenter for off-axis targets in X and Z directions

Table displacements determination

The mechanical deviations produced for table movements with and without additional weight in the most distal positions are shown in Table 3. In all cases, the maximum deviation is no higher than 1 mm

MLC calibration

The positional error for the central leaves is shown in Figure 5. The maximum error is 0.47 for bank Y1 and 0.64 for bank Y2. In Table 4 are represented the deviations for Bayouth and Garden tests at different gantry angles. The automated analysis was done on Pylinac, as shown in Figure 6. The qualitative behavior of the MLC movements was evaluated on ImageJ [Figure 6]. In this

Table 3: Deviations produced in the table with and without additional weight

Test	Position at the top (index 4) deviation x/y/z	Position at the bottom (index 45) deviation x/y/z
Without weight	0.4/0.3/–0.5	0.5/–0.1/0.1
With weight	0.4/0.7/–0.3	0.4/0.0/0.2

Table 4: Maximum deviation calculated for picket fence tests at different gantry angles

Test	Gantry angle (°)	Maximum deviation (mm)
Bayouth	0	0.202
Garden	0	0.238
Garden	90	0.236
Garden	180	0.256
Garden	270	0.307

case, we observed exact positioning of the leaves throughout their entire length, the profile obtained did not present peaks or valleys. The presence of a peak in the profile is an indication that the leaves are retracting from the correct position and the presence of valleys implies that the analyzed leaves are being advanced.

MR to MV coincidence isocenter

The baseline isocenter coincidence between the MRI and MV images was found to be −0.09, 4.11, and −0.23 mm in the X, Y, and Z directions, respectively

Imaging tests
Las Vegas test

There were detected 20 circles, higher than the tolerance established for MV images.

MR image quality

The analysis for MR image quality while the components of the linac were on/off is shown in Table 5. In all cases, the measured values are in agreement with the tolerances.

Magnetic resonance imaging geometric distortion

The distortion for diameter spherical volumes of 200, 300, 400, and 500 mm was 0.4, 0.7, 1.3, and 2.3 mm, respectively. These values are in accordance with the tolerances established by the vendor.

The distortion measured using QUASAR™ MRI3D are in accordance with tolerances established by the vendor in all cases, passing 98.4% of the control points with maximum, and mean deviation, for 200-mm diameter ROI, 0.99 mm, and 0.56 mm, respectively, and for 340-mm, 2.00 mm, and 0.60 mm.

Dosimetrical tests

Beam data collection

The measured profiles were in accordance with the TPS profiles in 100% of the cases. The average and minimum gamma passing rates (GPR) were 99.9% and 95.1%, respectively. The case of the minimum GPR was a profile with the irradiated field of 16 × 16 cm2 and a depth of 1.3 cm for gantry angle 270°. Regarding the independent Monte Carlo model, the maximum difference was 1.3% at depth 12 cm, neglecting the build-up region, as shown in Figure 7.
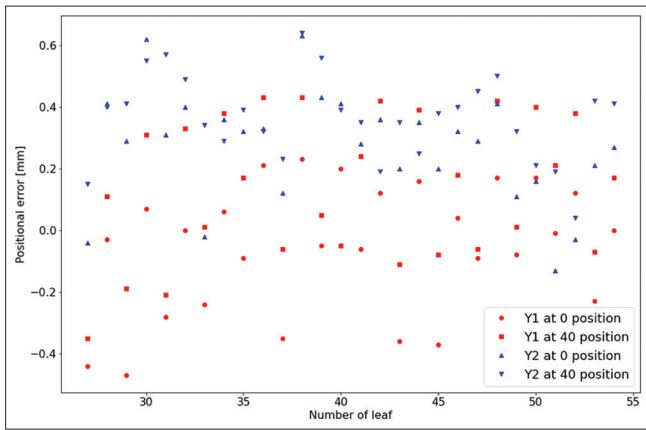

Figure 5: Positional errors determined for central leaves for two banks Y1 and Y2

Reference dose

The dose calibrated by the institution in a water phantom at a depth of 5 cm was 300 cGy. In contrast, the dose measured by the MDACC RDS was 299 cGy. An agreement within ± 5% was considered a satisfactory check

Beam quality

The TPR (20,10) measured with ionization chamber and solid water slabs, IC profiler®, and by the TRS-398 formula were 0.704, 0.705, and 0.704, respectively. The maximum variation between these values was 0.15%. This value is in agreement with the reported by Snyder *et al.*[11]

Output factors

The comparison of output factors measured with Semiflex and MicroDiamond is shown in Figure 8. It is important to note that for field sizes lower than 2 cm × 2 cm, the differences are higher than 10% regarding TPS values. The differences are reduced applying the correction factors established in TRS-483. However, these factors have to be considered only as guidance due to in TRS-483, the correction factors are described only for chamber non-MR compatible.

MLC transmission and dosimetric leaf gap

The transmission for MLC Y1 and Y2 banks was 0.25% on average, and for TPS was 0.60%. The DLG was equal to 0.271 mm. It was determined by the equations reported in Figure 9.

Dosimetry on inhomogeneities

The calculated doses on the homogeneous and inhomogeneous phantoms were 198.8 cGy and 217.6 cGy, while the measured doses were 199.2 cGy and 225.5 cGy, respectively. The maximum difference was 3.50% for inhomogeneous media
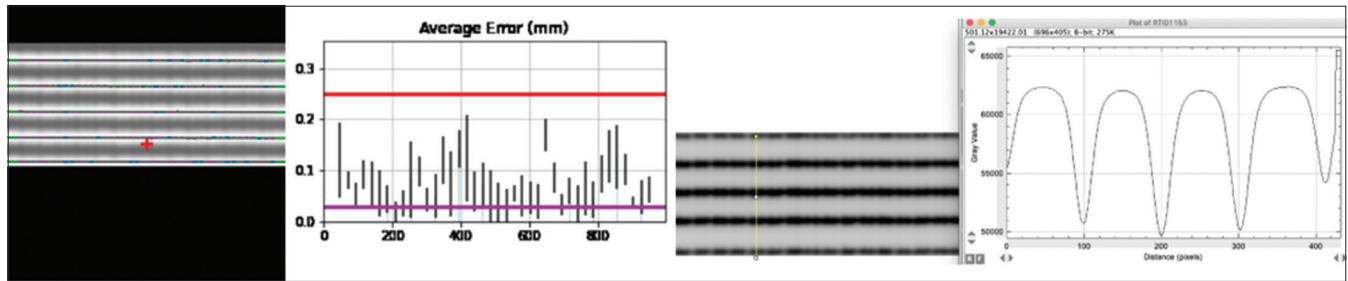

Figure 6: Analysis of the garden tests by Pylinac and ImageJ

Table 5: Flood field uniformity, slice profile, and spatial linearity and resolution evaluation maintaining the components of the linac on/off

Description	Parameter	Tolerance	Linac off	Linac on	Gantry	MLC
FFU	Nema S/N (B)	>59	73.28	72.43	72.72	74.25
	Nema_Int_Unif (%)	<47	39.07	39.19	39.82	39.76
SPL	Nema_perc_dif (%)	<0.5	0.12	0.15	0.20	0.17
SLP	Nema_FWHM (mm)	4.65–5.15	4.94	4.91	4.94	4.91
	Nema_Slice_Int (mm)	4.85–5.35	5.06	5.02	5.08	5.01
SPR	Hor/ver_pxl_size (mm)	<1.5	1.32	1.40	1.37	1.33

FFU: Flood field uniformity, SPL: Spatial linearity, SLP: Slice profile, SPR: Spatial resolution, MLC: Multileaf collimator
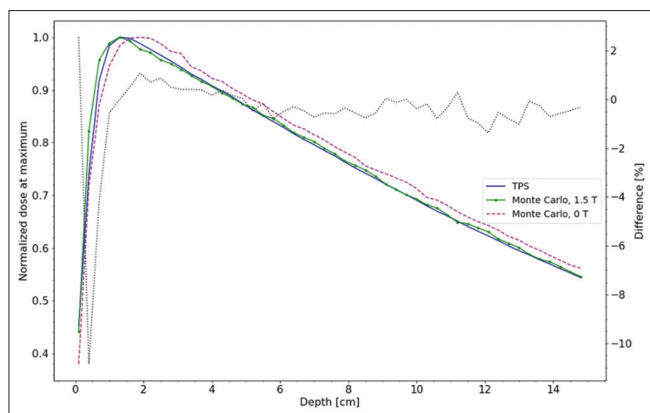
Figure 7: Comparison of treatment planning system dose profile in depth and an independent Monte Carlo model

Figure 8: Output factors measured with Semiflex and MicroDiamond on the axis and the differences taking as reference the treatment planning system values

Cryostat and table dose attenuation

The cryostat attenuation is 1.2% for all gantry angles. The higher bridge and table attenuation is 10% and 24%, respectively for angles between 110°-140° and 210°-240°, as shown in Figure 10.

Output versus gantry angle

The attenuation produced by bridge and table is considered in the TPS by the use of the couch model. The discrepancy between measurement and calculation of these components was evaluated as much as 2.51%, as shown in Table 6, and they are in agreement with the values reported for Snyder *et al*.[11] The difference higher than 1% at 270° was re-evaluated changing the geometry of the test using a cubic phantom giving a value of 0.995. Thus, this effect could be related to the setup of the ArcCheck® or to the contouring process.

IMRT commissioning

The passing rates were higher than 97%, for the criteria 3%/2 mm and 2%/2 mm and 94% for the more restrictive criteria of 2%/1 mm, as shown in Table 7.

End-to-end test

The dose difference for ATP and ATS strategies was -0.02% and 0.78% regarding TPS calculated dose. The measured dose was corrected by $k_B = 0.989$, $k_{PT} = 1.004$, and $k_{Q, Q0} = 0.986$.

DISCUSSION

The MRlinac Unity has adaptive radiotherapy delivery capabilities by integrating 1.5 T MR to acquire image before, during, and after each treatment. The aim of this concept is enabling the possibility to perform daily planning and soft tissue verification position.[21] Due to the novelty of this technology that offers different characteristics to conventional linacs, the system must be carefully commissioned in order to reach an appropriate accuracy. As a part of installation, although Unity lacks a formal Device Acceptance Test, Elekta provides a multidisciplinary team to perform some tests, and these tolerances enable Elekta Unity for clinical use. The procedures followed by Elekta are based on their golden beam data, which
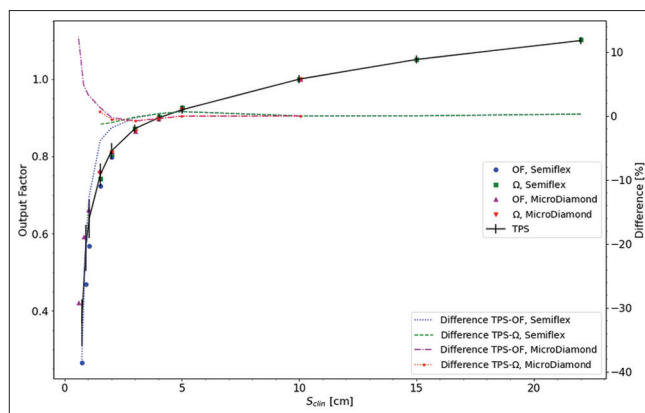
Table 6: Relationship between gantry angle and the dose measured with ArcCheck®

Gantry angle (°)	Relative measured value	Relative calculated value	Difference (%)
0	1.000	1.000	0.00
45	1.007	1.004	0.21
90	1.004	1.007	−0.36
135	0.837	0.857	−2.42
180	0.906	0.923	−1.89
225	0.840	0.861	−2.51
270	1.003	1.015	−1.11
315	1.007	1.012	−0.47

Table 7: Gamma passing rates for different criteria applied to the intensity-modulated radiation therapy plans

Plan	GPR for criteria of 2%/2 mm	GPR for criteria of 3%/2 mm	GPR for criteria of 2%/1 mm
10×10 field size	97.8	99.1	96.6
C-shape	98.3	98.8	94.3
Head-and-neck	97.8	99.3	95.0
Abdominal	98.6	99.4	96.2
Rectum	98.3	99.4	95.9
Prostate	98.2	99.4	93.7

GPR: Gamma passing rates

results in reduced commissioning time, and dosimetric errors generated in the configuration of the TPS by the medical physicist (MP) of the hospital. However, it is important to note that it is the responsibility of the MP to validate and approve each of the procedures to be in accordance with national regulation[6] and recommendation of AAPM task groups.[3,4] In order to verify and revise parameters out of tolerance, beam data collection and physics onsite testing was conducted jointly between Elekta team and the MPs of the hospital.

This validation has improved knowledge and confidence for clinical staff toward the use of the MRlinac, as well as the

application of strict criteria in mechanical and dosimetric tolerances for the linac, which will be the baseline values for daily, weekly, monthly and annual quality tests. It is important to note that wide baseline tolerances can cause, for example, that small variations in the mechanical isocenter avoid the use of the linac for specialized treatments, such as intra and extracranial radiosurgery (SRS, SBRT).

This work describes the good agreement with recent studies[11,12] in which mechanical, imaging and dosimetrical tests were evaluated. In addition to tests recently published, an analysis of MV off axis isocenter deviation was carried out, moving CCT along x and z directions. We reported a maximum deviation of 0.88 mm in a study range of 3 cm along the z axis. This value measured differs from Elekta recommendation up to 0.3 mm, due to Elekta highlights that the isocenter precision is lower than 0.5 mm. However, this result showed accordance within the tolerance allowed for quality controls performed for SRS/SBRT treatment lower than 1 mm, as established in TG-142. Thus, all measurements fully comply with NOM-033-NUCL-2016 in terms of radiation protection for linac operation[6] where it established tolerances up to 2 mm, and 2% for mechanical and dosimetrical tests, respectively. Additionally, the measurements pass Elekta recommendations in all cases. The Elekta tolerances are described in Supporting Information.
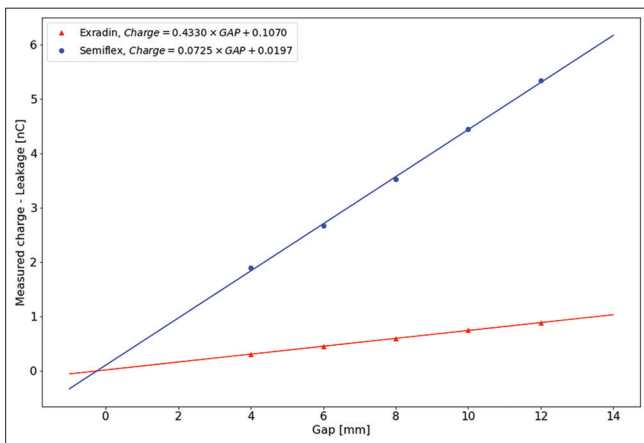
SBRT is a radiotherapy technique that allows high precision in delivery of high dose radiation to small targets. American Society for Radiation Oncology and American College of Radiology recommend to establish strict protocols for quality assurance applied to this technique.[22] The commissioning of IMRT treatment, we determined that it is possible to reach a GPR higher than 95% for 2%/2 mm DTA, complying with SBRT tolerances.[3] On the other hand, it is important to be aware that for field size smaller than 2 cm, the deviation differences for the output factor are higher than 10% [Figure 7] regarding TPS values, therefore future research in small field dosimetry with Elekta Unity is recommended before its clinical use for intracranial SRS or for small lesions.

It is of interest to highlight that this work can be useful to guide groups in Latin America, where new equipment with this technology is being installed and their acceptance and commissioning process are similar. This work shows that additional effort must be realized during the commissioning of Elekta Unity in order to satisfactorily comply with the applicable tolerances for performing SBRT treatments. This additional effort has a great impact, since there are needs to increase radiosurgery techniques in Latin America countries. This need arises from the lack of linacs in the region and the excessive workloads, limiting the use of SRS/SBRT techniques, where it has been demonstrated that they have clinical and operational advantages. Therefore, this facility opens access to advanced radiotherapy treatments in the northwest region of Mexico.

Conclusion

In this work, we performed the commissioning tests of the MRlinac Unity, including mechanical tests such as the positioning of the leaves using the Bayouth and Garden tests at different gantry angles, the DLG was measured, the deviations measured for targets off-axis, and in dosimetric terms the radiation beam model was verified with an independent Monte Carlo one, the output factors were obtained for large fields up to small fields of 0.5 cm, and differences >10% for small fields are reported, so precautions must be taken to treat lesions smaller than 2 cm in this unit. The dose was measured in the presence of inhomogeneities, and the attenuation produced by the components of the treatment table.
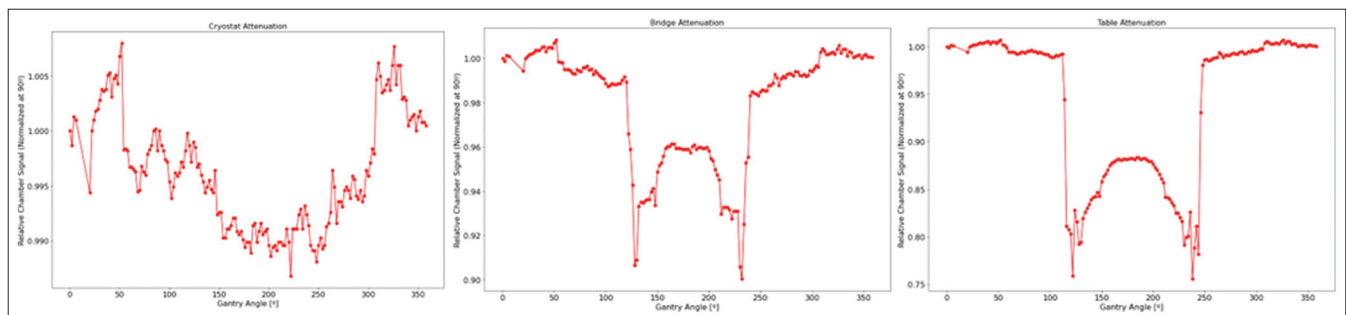

Figure 9: Measured charge versus the multileaf collimator (MLC) gap to determine the dosimetric leaf gap

Figure 10: Attenuation for cryostat, bridge and table in relation to gantry angle

The measurements confirm that the unit is in agreement with what was reported by other authors and that the tolerances established as a baseline allow a simpler migration to SBRT treatments in this machine, which can have a positive impact on the radiotherapy service and for the patients.

Conflicts of interest

There are no conflicts of interest.

REFERENCES

1. Corradini S, Alongi F, Andratschke N, Belka C, Boldrini L, Cellini F, *et al*. MR-guidance in clinical reality: Current treatment challenges and future perspectives. Radiat Oncol 2019;14:92.
2. Raaijmakers AJ, Raaymakers BW, Lagendijk JJ. Magnetic-field-induced dose effects in MR-guided radiotherapy systems: Dependence on the magnetic field strength. Phys Med Biol 2008;53:909-23.
3. Klein EE, Hanley J, Bayouth J, Yin FF, Simon W, Dresser S, *et al*. Task group 142 report: Quality assurance of medical accelerators. Med Phys 2009;36:4197-212.
4. Ezzell GA, Burmeister JW, Dogan N, LoSasso TJ, Mechalakos JG, Mihailidis D, *et al*. IMRT commissioning: Multiple institution planning and dosimetry comparisons, a report from AAPM task group 119. Med Phys 2009;36:5359-73.
5. Keall PJ, Glide-Hurst CK, Cao M, Lee P, Murray B, Raaymakers BW, *et al*. ICRU REPORT 97: MRI-Guided Radiation Therapy Using MRI-Linear Accelerators. Journal of the ICRU 2022;22:1-100. doi:10.1177/14736691221141950.
6. NORMA Oficial Mexicana NOM-033-NUCL-2016. The official name has to be in Spanish due to is a official law. Available from: https://www.dof. gob.mx/nota_detalle.php?codigo=5446806&fecha=04/08/2016#gsc. tab=0. [Last accessed on 2023 Nov 16].
7. International Atomic Energy Agency, Code of Practice TRS 398. Absorbed dose determination in external beam radiotherapy: An international code of practice for dosimetry based on standards of absorbed dose to water. 2001. Available from: https://www.iaea.org/es/ publications/7207/determinacion-de-la-dosis-absorbida-enradioterapia-con-haces-externos.
8. International Atomic Energy Agency, Code of Practice TRS 483, Dosimetry of Small Static Fields Used in External Beam Radiotherapy, Vienna; 2017. Available from: https://www-pub.iaea.org/MTCD/ Publications/PDF/D483_web.pdf. [Last accessed on 2024 Mar 19].
9. de Pooter J, Billas I, de Prez L, Duane S, Kapsch RP, Karger CP, *et al*. Reference dosimetry in MRI-linacs: Evaluation of available protocols and data to establish a code of practice. Phys Med Biol 2021;66:05TR02.
10. Powers M, Baines J, Crane R, Fisher C, Gibson S, Marsh L, *et al*. Commissioning measurements on an elekta unity MR-linac. Phys Eng Sci Med 2022;45:457-73.
11. Snyder JE, St-Aubin J, Yaddanapudi S, Boczkowski A, Dunkerley DA, Graves SA, *et al*. Commissioning of a 1.5 T Elekta unity MR-linac: A single institution experience. J Appl Clin Med Phys 2020;21:160-72.
12. Roberts DA, Sandin C, Vesanen PT, Lee H, Hanson IM, Nill S, *et al*. Machine QA for the Elekta unity system: A report from the Elekta MR-linac consortium. Med Phys 2021;48:e67-85.
13. Rahman MM, Lei Y, Kalantzis G. QALMA: A computational toolkit for the analysis of quality protocols for medical linear accelerators in radiation therapy. SoftwareX 2018;7:101-6. [doi: 10.1016/j. softx.2018.03.003].
14. Low DA, Li Z, Drzymala RE. Minimization of target positioning error in accelerator-based radiosurgery. Med Phys 1995;22:443-8.
15. Ali Z, Adili M, Bamajboor S. Pylinac: A toolkit for performing TG-142 QA related tasks on linear accelerator. Phys Medica 2016;32:292-3. doi:10.1016/J.EJMP.2016.07.122.
16. Rojas-López J, Chesta M, Venencia C. Experimental determination of set-up displacements in anthropomorphic phantom in single-isocentre radiosurgery for multiple brain metastases by off-axis Winston – Lutz test: ExacTracTM v. 6 versus DynamicTM. J Radiother Pract 2023;22:E72.
17. Venencia CD. PhD thesis. 2012. Quality Assurance of the Physical Aspects of Advanced Technology in Radiotherapy, International Atomic Energy Agency -Coordinated Research Project E2.40.15. Facultad de Matemática, Astronomía, Física y Computación, Universidad Nacional de Córdoba. Available from: https://www. famaf.unc.edu.ar/documents/1024/DFis164.pdf. [Last accessed on 2023 Nov 18].
18. Gayol A, Vedelago J, Valente M. MRI-LINAC dosimetry approach by Monte Carlo codes coupling charged particle radiation transport with strong magnetic fields. Radiat Phys Chem 2022;200:110171.
19. Andreo P, Burns DT, Kapsch RP, McEwen M, Vatnitsky S, Andersen CE, *et al*. Determination of consensus k (Q) values for megavoltage photon beams for the update of IAEA TRS-398. Phys Med Biol 2020;65:095011.
20. O'Brien DJ, Sawakuchi GO. Monte Carlo study of the chamber-phantom air gap effect in a magnetic field. Med Phys 2017;44:3830-8.
21. Winkel D, Bol GH, Kroon PS, van Asselen B, Hackett SS, Werensteijn-Honingh AM, *et al*. Adaptive radiotherapy: The Elekta Unity MR-linac concept. Clin Transl Radiat Oncol 2019;18:54-9.
22. Chao ST, Dad LK, Dawson LA, Desai NB, Pacella M, Rengan R, *et al*. ACR-ASTRO practice parameter for the performance of stereotactic body radiation therapy. Am J Clin Oncol 2020;43:545-52.

SUPPORTING INFORMATION

Elekta reccomendations for Unity

Gantry angle: 0.1 degree

MV iso: 0.5 mm

MV off-axis: N/A

Table displacement: 1 mm

MLC: 1 mm

MRtoMV: 1 mm from baseline

Las Vegas: Baseline

PIQT and MRI geom distortion: See attached at the bottom

MCU comparison: 95% gamma 2%/2 mm (dejando fuera buildup y las zonas con D <20% en los perfiles)

Reference dose: 1%

Beam quality: Within 1% of 0.700

OF: Baseline

MLC transmission: <0.5%

Output veraus GA: <1% (with the exception of the zones across the table due to limitations in the Monaco model)

IMRT: Gamma 3%/2 mm global >95%

EndToEnd: dif <3%

TABLE VII. Periodic Image Quality Test (a) Sequences, FFE-Fast Field Echo, SE-Spin Echo, TE-Echo time, TR-Repetition time and (b) Test Criteria.

(a)

Scan name	QA1	QA2	QA3
Scan mode	Multi-slice	Multi-slice	2D
Scan technique	SE	FFE	SE
Receive coil	MRL Ant/Post	MRL Ant/Post	Body
TE (ms)	30/100	15	3*50
TR (ms)	1000	200	1000
Voxel size (mm^3)	1.2/1.2/5.00	1.2/1.2/5.00	0.98/0.98/15.0
Slices	Noise, SPL, FFU, SLP, SPR	SPL, FFU, SLP	FFU

(b)

Test	Scan name	Specification	Acceptance level
Flood field uniformity	QA1 (echo 1, 2)	NEMA Signal to Noise[a] NEMA Integral Uniformity[a]	> 59, >44 < 47, <48
	QA2	NEMA Signal to Noise[a] NEMA Integral Uniformity[a]	>48 <47
	QA3 (echo 1, 2, 3)	NEMA Signal to Noise[a] NEMA Integral Uniformity[a]	>45, >39, >30 <10, <10, <10
Spatial linearity	QA1	Differential linearity (35 points)	< 0.5
Slice Profile	QA1 (echo 1, 2)	NEMA Full width at half maximum (mm) NEMA Slice Integral (mm)	4.65-5.15, 4.45-4.95 4.85-5.35, 4.65-5.15
	QA2	NEMA Full width at half maximum (mm) NEMA Slice Integral (mm)	4.75-5.25 4.9-5.4
Spatial resolution	QA1 (echo 1, 2)	Horizontal pixel size Vertical pixel size	<1.3 mm, <1.3 mm <1.5 mm, <1.5 mm

Suggested limits do not relate to machine performance specifications. These are provided as guidance to a "minimum" expected performance.
[a]Positioning and size of ROIs differ to NEMA standard and are specific to the 200 mm Philips phantom.